Evidence for chaotic behavior in driven ventricles

Guillermo V. Savino,* Lilia Romanelli,‡ Diego L. González,§ Oreste Piro,§ and Max E. Valentinuzzi*
*Bioingeniería, Instituto Superior de Investigaciones Biológicas (INSIBIO), Consejo Nacional de Investigaciones Científicas y Técnicas (CONICET), and Universidad Nacional de Tucumán (UNT), Tucumán; ‡Centro Argentino de Estudios de Radiocomunicaciones y Compatibilidad Electromagnética (CAERCEM), Buenos Aires; and §Departamento de Física Teórica, Universidad Nacional de La Plata (UNL), La Plata, Argentina

ABSTRACT Toad ventricles were externally driven by periodic pulses while monophasic action potential (MAP) signals were recorded in seven excised and seven in situ ventricles. As the frequency was slowly increased in steps, the stimulated tissue displayed several dynamic characteristics. Hierarchies of periodic behavior, like phase-locking and period-doubling sequences leading to chaos, were observed. Results showed that subharmonic bifurcations (order one and two) and chaotic-like behavior may systematically occur in the MAP signal within a definite frequency interval in the 1:1 phase locking regime. The chaotic, or more cautiously expressed, chaotic-like behavior is characterized by the power spectrum, the autocorrelation function, the Poincaré map, and the reconstructed 2-D phase portrait. It is concluded that (*a*) bifurcations of order one and two and the characteristic irregular behavior are evidences of local universal chaotic dynamics in cardiac tissue; (*b*) there are no qualitative differences in the dynamics of the in situ and excised ventricles; and (*c*) fibrillation seems to be related to chaotic behavior, but whether they are similar or equivalent phenomena still remains to be seen.

INTRODUCTION

Many efforts have been devoted to elucidate the electrophysiological mechanisms involved in cardiac tissue dynamics. At least two basic mechanisms may account for the onset of rapid ventricular arrhythmias: reentry and transformation of nonpacemaker fibers into pacemaker ones (1).

At the present time, new electrophysiological behaviors have been described in nerve and cardiac tissue. Best (2) found phase resetting and annihilation caused by a single pulse during rhythmic firing regime of the Hodgkin-Huxley model due to constant current application. The same phenomena in spontaneous rhythmic isolated cardiac pacemaker cells were found by Jalife and Antzelevitch (3). Phase resetting, annihilation, and chaotic dynamics are closely related phenomena (4). This kind of behavior was also found by numerical simulations in the Beeler and Reuter model of cardiac action potential in the presence of periodic stimulation or when suitable depolarizing constant currents were injected (5–7). The same dynamics were described and widely studied in solvable models of relaxation oscillators, which allow a complete geometrical understanding of the problem (4, 8–11). Experiments on cardiac tissue have also shown chaotic dynamics using self-oscillating cells, or aggregates of cells, externally perturbed by periodic pulses (12). Alterations in clinical electrocardiographic records due to nonlinear cardiac dynamics poses a major problem yet to be solved. There is a growing interest in the application of nonlinear models to some of the rapid ventricular arrhythmias. Ritzenberg (13) reported evidence of nonlinear behavior (period demultiplying regime or, as proposed by these authors, "period multupling") in the electrocardiogram and arterial blood pressure traces from the noradrenaline-intoxicated dog. Besides, Goldberger (14) studied the ECG and epicardial electrogram frequency spectra during fibrillation in an effort to find out whether fibrillation is "chaos."

This paper intends to analyze whether rapid, induced cardiac rhythms can be described by nonlinear chaotic-like models. If this is the case, at least one route to chaos should be identified in some observable variable or parameter, and thus the irregular behavior could be defined as "chaotic." The cardiac monophasic action potential (MAP) is taken as the basic raw signal, and its behavior will be considered as chaotic if (*a*) it is preceded by period-doubling bifurcations, (*b*) the power spectrum displays broad band noise in the low frequency region, (*c*) the autocorrelation function decays rapidly, (*d*) the Poincaré map shows space-filling points, and (*e*) the phase-portrait in the bidimensional space presents characteristics similar to other known chaotic attractors.

MATERIALS AND METHODS

Experimental set-up

Pacing stimuli of increasing frequency were applied to 14 *Bufo arenarum* ventricles (mean weight, 3.5 g; SD = 1.0). Seven ventricles were removed and perfused with Ringer solution using a cannula. To do this, we fixed the ventricles to the cannula by a ligature at the level of the

atrioventricular junction and maintained them at room temperature (20°C). Under these conditions, the ventricles generally stopped; exceptionally, they discharged at very slow rate in an erratic fashion. The stimulator was then turned on and pacing began at low frequency (10 ppm) and slowly increased in steps (Fig. 1).

The other seven ventricles were exposed in situ (spontaneous rate, ~25 ppm). The applied stimulus frequency was slowly stepped up, beginning at 60 ppm, and removed when fibrillation or evident desynchronization was obtained. This was repeated twenty times in each animal. In both cases, in situ and excised ventricles, the periodic stimuli were applied near the base of the ventricles by means of two fine nichrome wires inserted very close to each other. Stimulus amplitude was fixed at twice the capture threshold (3 mA), and duration was fixed at 2 ms. A model 588 stimulator (Grass Instrument Co., Quincy, MA) was used together with stimulus isolation and constant current units. Surface electrocardiogram (ECG) and monophasic action potentials (MAP) were recorded on a polygraph (model 2600S; Gould Inc., Santa Clara, CA). The MAP signal (15, 16) was obtained with a suction electrode (external diameter, 1 mm) applied on the epicardial surface of the ventricles. In all cases, this electrode was placed 5 mm apart from the stimulating one. Such distance is sufficiently far off to ensure almost no influence of electronic spread because the length constant of frog cardiac tissue is in the order of 0.385 mm (17). Shanne and Ruiz Ceretti (18), in their book, collected a number of length constant values reported in the literature. The range for cardiac tissue (ventricle and atrium) in different species goes from a minimum of 0.05 mm up to 2.6 mm, with an average of 0.93 mm (SD = 0.71) calculated by us over 14 values taken from a table published by these authors. Thus, perhaps we should consider 1 mm as a good representative value for the cardiac tissue length constant. Even so, the influence at 5 mm of the electrotonic spread is negligible. Also, the MAP signal was visualized and stored in a oscilloscope (model T912; Tektronix, Inc., Beaverton, OR). In seven cases (three in vivo and four perfused), this signal was digitalized and stored in a computer disk to perform statistical analysis. Digitalization was carried out by taking 20,000 samples, one every 2 ms during 40 s, with an A/D converter. The MAP signal was distorted by the superposition of the electrocardiographic artifact (ECG) which was, as a rule, less prominent in the records with the larger MAP amplitude. In all cases, we tried to minimize the ECG artifact. Fig. 1 summarizes the experimental set-up, both for the excised and in situ cases. Fig. 2 shows the ECG (*A*) and the MAP signal (*B*) from an in situ heart, obtained simultaneously. In this situation, the amplitude and duration parameters of the MAP can be easily measured. Observe that the base line displacement is small. In all the experiments, attention was focused on observing periodic differences in the MAP amplitudes, its stability, and repeatability.

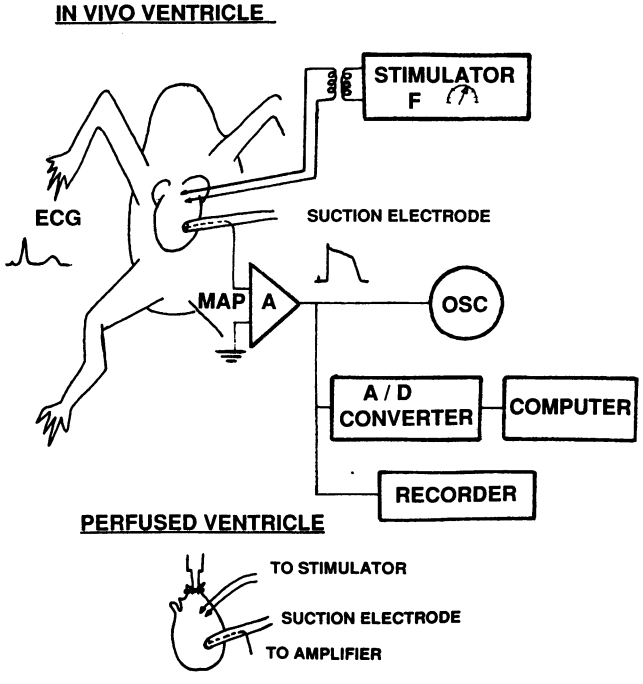

FIGURE 1 Experimental set-up. (*Top*) For the in vivo ventricle. (*Bottom*) For the perfused ventricle. The stimulator was isolated and its frequency was verified by measuring with an oscilloscope (not shown) the applied stimulus period. Besides, readings were also made on the instrument dials (model S88; Grass Investment Co., Quincy, MA). The monophasic action potential (MAP) was sent to an oscilloscope (OSC) and also to the A/D converter (a laboratory custom-made equipment) and a graphic recorder (model 2600S; Gould Inc., Santa Clara, CA). The electrocardiogram (ECG) was obtained from simple subcutaneous needle leads.

Signal processing

Power spectra and autocorrelation values were calculated from 40 s (20,000 data points) pieces of stable MAP signal runs to detect periodic behavior and to qualitatively characterize its irregular nature. Power spectra calculation was repeated twice to assess the stability of the signal, first for the overall 40-s piece, then for the first 20 s, and finally for the second 20 s. Stable behavior was assumed when all three calculated spectra along with the recorded MAP temporal series showed no changes. Besides, we recorded the maximum MAP amplitude, $\hat{X}_i$, for each beat by taking the difference between the peak value and the base line previous to each stimulus artifact.

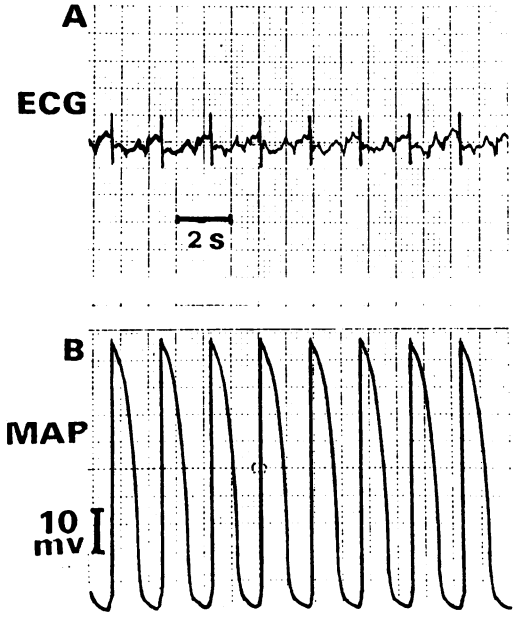

FIGURE 2 (*A*) Surface electrocardiogam (ECG). (*B*) Monophasic action potentials (MAP) from toad ventricle. Frequency: 33 ppm. MAP duration: 1 s. MAP amplitude: 61 mV.

Nonperiodic behavior of the MAP signal perhaps could be characterized by a chaotic attractor due to some observed features of deterministic chaos. Taking this possibility into account, bidimensional phase portraits were reconstructed by means of the embedding technique (19–21), starting with the MAP temporal series to (*a*) assess their structure, and (*b*) estimate the sensitivity to the initial conditions presented by the system.

A phase portrait is the set of trajectories in the phase space, for a given set of control parameters, for all the possible initial conditions of the system. By and large multidimensional, it contains considerable information. Suffice it to say that a single point fully characterizes the whole system at a given instant.

For an observable $X(t)$—the MAP signal—and a delay T, an m-dimensional phase portrait is constructed with vectors of the type

$$\mathbf{X}(t) = \{X(t_k), \cdot X(t_k + T), X(t_k + 2T), \ldots X[t_k + (m-1)T]\},$$

in which $t_k = k\Delta t$, for $k = 1, 2, \ldots \infty$, and m is the embedding dimension. This portrait will have the same properties as the n-dimensional original phase portrait with n independent variables of the dynamic system under study (in our case, the ventricles). The condition $m \geq 2n + 1$ must be verified. The delay T can be arbitrarily chosen. We took it as equal to the time of the first zero crossing of the correlation function (see Results).

RESULTS

The 14 driven ventricles studied showed period-doubling sequences and phase-locking responses in the MAP amplitudes when the pacing rate was high. In Fig. 3, the amplitude period-doubling sequences of a perfused ventricle in 1:1 frequency locking regime are shown. In Fig. 3 *A*, at 88 ppm, a difference between successive crests of the MAP amplitude is not evident, but careful observation detects small differences. Nevertheless, if the frequency increased (from 88 to 97 ppm) the amplitude difference between succesive MAP crests is more evident, as in Fig. 3 *B*, where the amplitude difference between the *ab*, *ab*, series is ~4.3 mV, corresponding to a 9% amplitude change. In Fig. 3 *C*, the amplitude difference between the *a*, *b* waves of the MAP is ~6.4 mV (amplitude change 13%) at 102 ppm. However, in Fig. 3 *A–C*, there are only two different amplitudes indicated by *a* and *b*. This is a period two pattern (see also Table 1), the first period-doubling bifurcation, meaning that this is repeated at twice the stimulator period or half frequency (F/2). This might be interpreted as the first, or order one (2^1) amplitude bifurcation, in the 1:1 frequency locking regimen, which is observed in all cases within the interval of 90–110 ppm. Fig. 3 *D* shows a pattern of four different MAP amplitudes, a period four pattern, the second

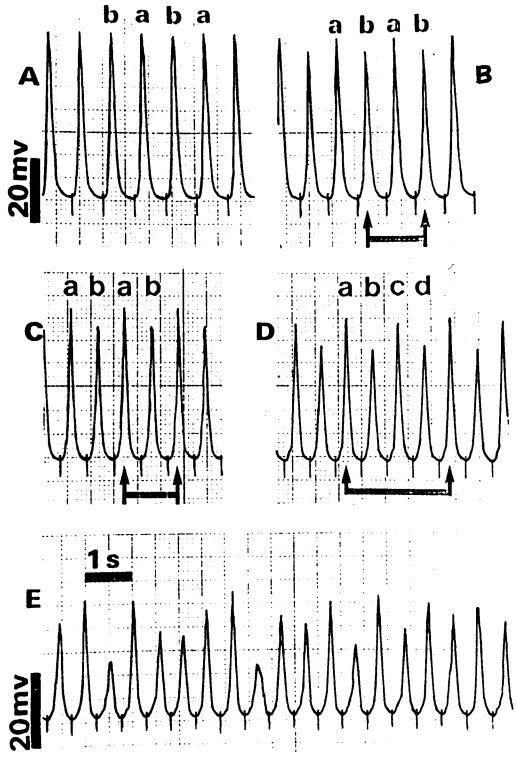

FIGURE 3 Period-doubling sequences and chaotic behavior of the MAP signal amplitude in the 1:1 frequency locking of a perfused toad ventricle. All the MAP signals are preceded by the stimulus artifact. Frequency increases from panel *A* (88 ppm) to *E* (113 ppm) (see text).

TABLE 1 Qualitative characterization of the map signal in the 1:1 phase-locking regime

Behavior	Driving frequency F: Perfused	Driving frequency F: In vivo	Periodicity	MAP time series pattern	Subharmonic frecuency spectrum	Correlation C (λ)	2D-trajectory number	Poincaré map
	ppm	*ppm*						
	<80	<200	Period 1		F	Continue	One	Single point
Periodic	80–100	210–240	Period 2		F; F/2	Oscillates	Two	Two points
	100–120	230–300	Period 4		F; F/2 F/4; 3F/4	Oscillates	Four	Four points
Nonperiodic	>120	>250	Cuasiperiodic or chaotic		Broadband noise	Decays quickly	Many bands	Many map-filling points

period-doubling bifurcation, indicated by the *a*, *b*, *c*, and *d* series. The period of this pattern is four times the stimulating period or quarter frequency (F/4). This might be interpreted as the second bifurcation or order two (2^2) bifurcation, and is observed within the interval of 100–120 ppm. The exponent gives the bifurcation order. A short frequency increase changes the pattern formerly observed into an irregular behavior, probably a higher order (2^n) bifurcation or chaotic behavior. In Fig. 3 *E* all the MAP amplitudes are different, i.e., there is no recognizable amplitude pattern.

The same phenomena formerly described in perfused ventricles were observed in in situ ventricles. In this case, the sinus venosus and the atria of the in situ heart did continue their beating. Nevertheless, no qualitative difference was detected in the observed period-doubling sequences. The frequency intervals were 210–240 ppm and 230–300 ppm for the period two and period four (first and second order bifurcations), respectively. Fig. 4 shows sequences of MAP amplitude period-doubling bifurcations for the in situ toad ventricle. In Fig. 4 *A*, the control and calibration MAP signals are displayed, the spontaneous rhythm was 30 ppm and the maximum MAP amplitude was 60 mV. The arrow indicates the beginning of stimulation. Fig. 4 *B* shows a period two. Only two MAP amplitudes alternate at twice the driving stimulator period (the period of this pattern is indicated by the bar between the arrows). The frequency of the stimulator was 250 ppm. This can be verified with the stimulus artifact. Also, the difference in the MAP amplitudes is ~2.8 mV (amplitude change 6.8%). At the same frequency but after 30 s, Fig. 4 *C* shows period four sequences. Now, four different MAP amplitudes are being repeated every four stimulator periods; the period of this pattern is indicated by the bar between arrows. These periodicities are sensitive to small driving frequency changes and show, by and large, good stability for several tens of seconds or even minutes. In Fig. 4 *D*, an irregular aperiodic amplitude variation in the 1:1 regime was established at 300 ppm. In principle, no pattern can be recognized. When the frequency was slightly increased (Fig. 4 *E*), the MAP signal desynchronized and looked like fibrillation.

Fig. 5, *A* and *B*, illustrates periodic behaviors of periods 2 and 4, respectively. The corresponding spectra depict maxima at F and F/2 (for period 2) and F, F/4, F/2, and 3F/4 (for period 4). Fig. 5 *C* describes the irregular behavior. Maxima were replaced by a noise band in the low frequency side (frequencies lower than the pacing one). Nontheless, and due to the 1:1 phase-locking, the pacemaker frequency (2 Hz) appears as a peak in the power spectrum. Appearance of these frequencies suggest a route to chaos via period-doubling bifurcations.

Fig. 6 is a bidimensional phase portrait during the

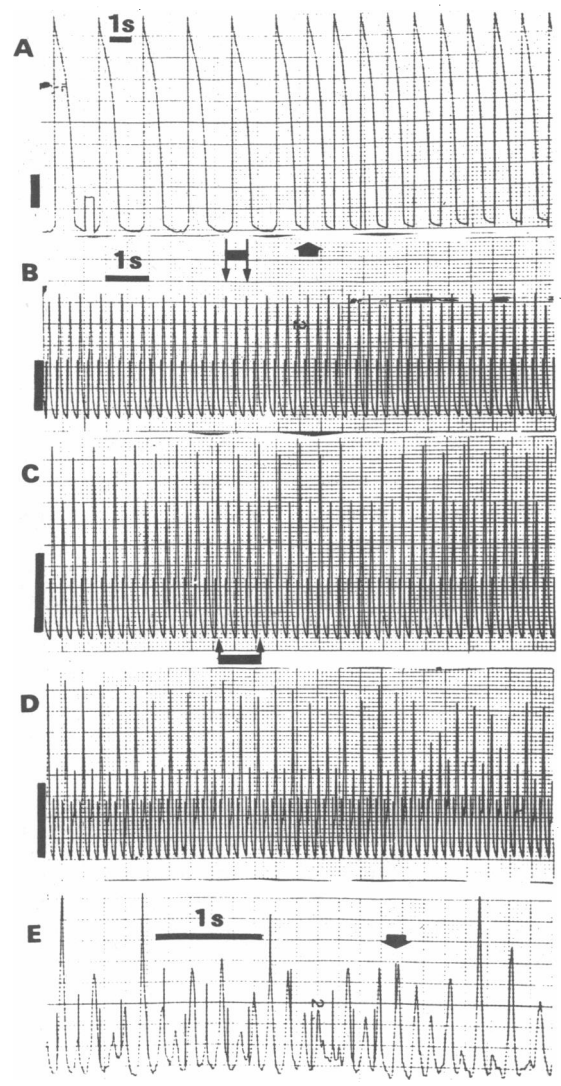

FIGURE 4 Period-doubling sequences of MAP amplitude in in situ ventricles. Control MAP signals are shown in *A*. At the arrow, the stimulator was connected and the stimulus signal appears superimposed to the upstroke of the MAP. The amplitude calibration (rectangular pulse after the first beat in *A*) is 10 mV. Time scale is the same for *B*, *C*, and *D*.

MAP time series irregular behavior reconstructed by means of the embedding technique (19). It shows the intersection between the two-dimensional orbits and the indicated straight line (Fig. 6, *dashed line*). Intersection points $\hat{X}_i$ are used to construct the Poincaré map in the plane $\hat{X}_{n+1}$ versus $\hat{X}_n$. To obtain greater differences, this line was adjusted according to the maxima, $\hat{X}_i$, of the MAP signal. Under these conditions, the Poincaré map for maxima is obtained by simply plotting $\hat{X}_{n+1}$ versus $\hat{X}_n$. Fig. 7 shows such a map for the period 4 periodic solution obtained with 160 beats. Plotted values are indicated in Fig. 5 *B* as $\hat{X}_1$, $\hat{X}_2$, $\hat{X}_3$, and $\hat{X}_4$.

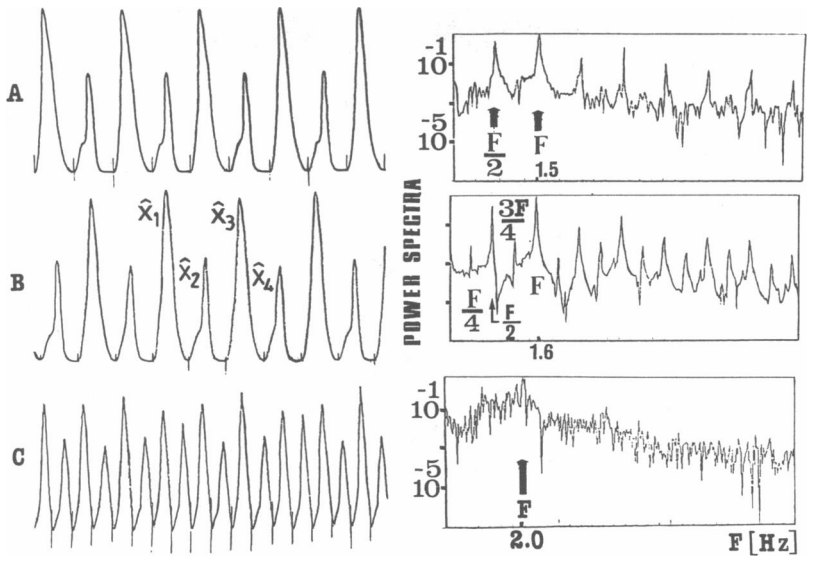

FIGURE 5 Time series reconstructed from the analogue MAP signal (perfused ventricle). By them, the corresponding power spectra are displayed. F, driving frequency.

Results of the tests performed to characterize periodic and nonperiodic behavior, in the 1:1 regime, are summarized in Table 1. Temporal MAP series are displayed to indicate the observed periodic patterns. The column labeled *Subharmonic frequency spectrum* gives those frequencies present in the power spectra shown in Fig. 5. The column *Correlation* displays the result of the autocorrelation calculation for the MAP amplitude $\hat{X}_i$. The autocorrelation did not change for period 1, oscillated around zero for periods 2 and 4, and decayed rapidly for the nonperiodic case. The column before the last summarizes the bidimensional phase portrait results. For the periodic case, there were separate orbits: one for period 1, two for period 2, and four for period 4. Orbits became bands in the nonperiodic case (Fig. 6). In all cases, near the stimulus artifact (*P* in Fig. 6), trajectories narrowed down to almost a line and, thereafter (~50 ms later), open up to become bands. This means that two consecutive beats with trajectories very close to each other before the stimulus will follow quite different paths, as indicated by

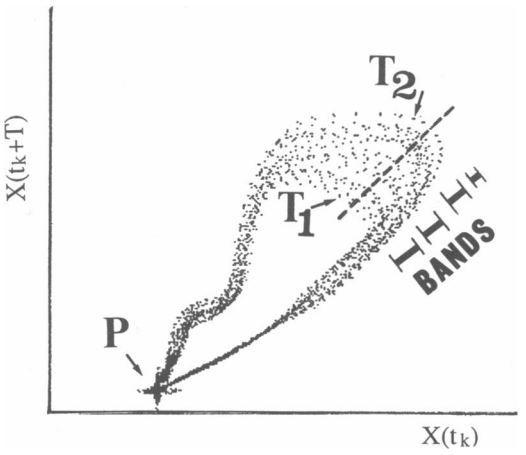

FIGURE 6 Two-dimensional projection, $\{X(t_k + T)$ versus $X(t_k)\}$ for $T = 20$ ms, of a likely higher-dimension chaotic attractor. It corresponds to the temporal series shown in Fig. 5 *C*. There are 180 superimposed beats. Point *P* indicates the stimulus artifact. T_1 and T_2 indicate two different trajectories originated at very close initial conditions right before *P*. Dashed line marks a Poincaré section.

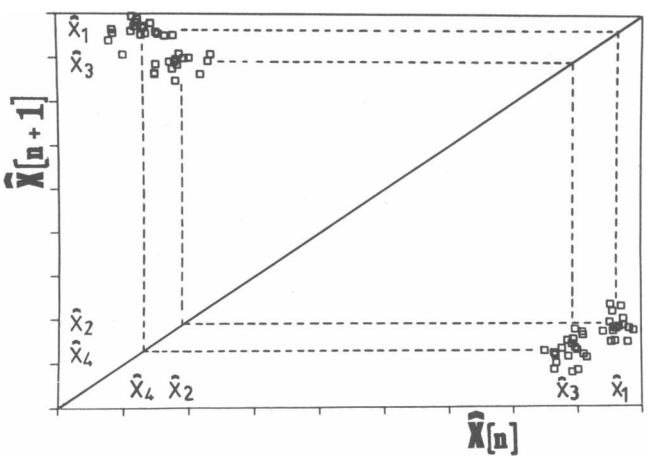

FIGURE 7 One-dimensional Poincaré map $\hat{X}_{n+1}$ versus $\hat{X}_n$ for period 4. There are 160 beats superimposed. Spread is likely due to inherent experimental noise.

T_1 and T_2. In other words, there is sensitivity to the initial conditions, a characteristic found in chaotic dynamic systems. Finally, the last column (Table 1) shows the number of points found in the Poincaré maps. There was one point for period 1 behavior, two for period 2, and four for period 4. When the behavior was irregular, many points filled the map. They could not be described by a parametric straight line, confirming the irregularity of the signal and suggesting a deviation from the unidimensional description. Fig. 7 illustrates a Poincaré map, $\hat{X}_n$ versus $\hat{X}_{n+1}$, for period 4 shown in Fig. 5 *B*, and shows the spread of the experimental points (indicated by open squares in the figure).

Fig. 8 *A–C*, shows the transition from 1:1 to 2:1 phase-locking response of the in situ paced ventricle. Fig. 8 *A* is a control strip. To the left of the arrow the natural rhythm is 33 ppm. Before each MAP, we can see the atrial activity. The arrow indicates the beginning of the stimulation and the pacemaker stimulus artifact is observed. As frequency increased, MAP amplitudes decreased and a transient alternans in the MAP durations can be observed. After the transient time, the MAP duration stabilized to a mean value. In Fig. 8 *B*, at 97 ppm frequency, big and small MAPs alternate periodically. The small MAP is shorter in duration and amplitude and is not preceded by a pause or diastolic period. These responses change in different ways, sometimes with a slight increase in frequency. The bigger MAP increased both its duration and amplitude. The smaller MAP is shorter in each cycle and finally was transformed into rapid oscillations. At the arrow, pacing was stopped. The oscillations persisted during 1.6 s, stopped, and the heart reassumed its normal rhythm. In Fig. 8 *C*, the same situation as in Fig. 8 *B* is illustrated, but in this case the smaller MAP did not go into rapid oscillations. Only one or two oscillations are seen in each cycle (right-hand part of record). The stimulator frequency in Fig. 8 *C* is also 97 ppm. At the arrow, the stimulus was removed and the heart reassumed its normal rhythm.

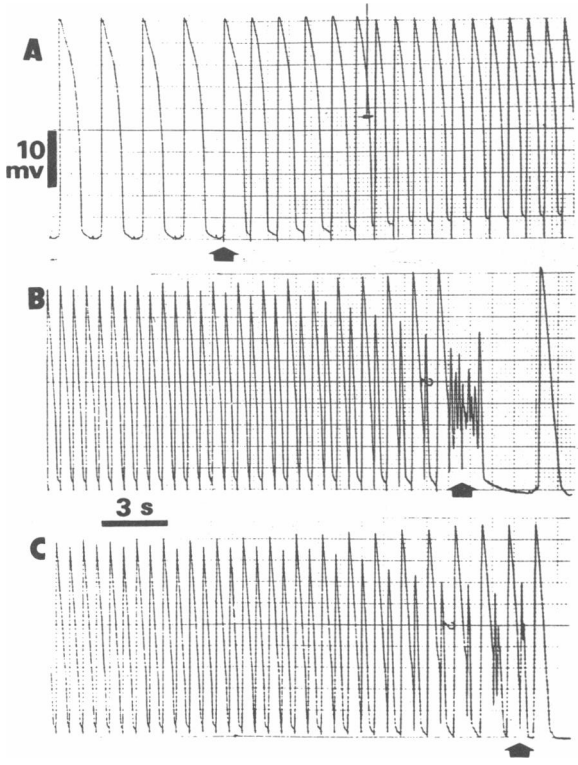

FIGURE 8 Phase-locking responses in MAP signals of toad ventricle. The initial situation (33 ppm) before and during the stimulation is shown in *A*. At the arrow, the stimulator was connected at 55 ppm. Panels *B* and *C* show the development of the responses at 97 ppm. In *B*, the change is interrupted by rapid oscillations. At the arrow the stimulator was removed. In *C*, the premature response changes to one or two rapid oscillations. Stimulator removed at the arrow.

DISCUSSION

These results would support the hypothesis of a low-dimensional chaotic attractor located in the simpler amphibian cardiac syncytium in which a route to chaotic behavior would appear by period-doubling bifurcation. The experiment we describe is a useful model to assess such possibility. The MAP signal, an extracellular but rather localized record, seems to be adequate to show the nonlinear dynamics of very small areas of cardiac tissue using driving frequencies at which other recording techniques (like surface ECG or direct electrogram) are not able to supply much information. Recording of the MAP signal is relatively easy to obtain, even from ventricles or atria during tachycardia. The signal-to-noise ratio is much better than with the ECG or the direct electrogram because the MAP signal from toad ventricle, at normal sinus rhythm, has an amplitude in the order of 60 mV. Special attention must be given to the input amplifier common mode rejection ratio (CMRR) to minimize the interference from the rest of the myocardium electrical activity. Toad ventricle is a good model for cardiac nonlinear dynamics due to its inherent tissue homogeneity and to the lack of coronary system, which are characteristics of lower species hearts. The pacing frequency as a control parameter is convenient, for it can be adjusted very slowly and finely in steps to detect bifurcations which appear within narrow ranges. Moreover, there is a direct correlation with those theoretical oscillators wherein the dynamics is studied by changing the driving frequency and amplitude. Changing the driving frequency allows a gradual approach to rapid arrhythmias and to disordered behaviors, as the case is in mammalian fibrillation. Similar rhythms can be induced in toad ventricles (22). The

described dynamics showed no change by increasing the suprathreshold stimulus amplitude.

The period 2 (or first period doubling bifurcation) was observed by other authors in the R and T waves of the ECG (23) during tachycardia and also in the electrogram and myogram of cardiac tissue. These sequences, with only two different amplitudes, were called alternans but no other significance was attributed to them. The second period-doubling bifurcation (or period 4) is not easy to obtain experimentally, probably because of (*a*) a narrow frequency interval, (*b*) low stability, and (*c*) very small differences between the amplitudes.

Higher order periodicities are very difficult to observe. We have detected other periodicities (as period 8) but not systematically. The period 4 was not detected in every trial; it could well be that the frequency increasing steps were too big to transfer the system directly to a high-order bifurcation or to a different *m:n* phase-locking regime. Nonetheless, the irregular behavior herein described as chaotic is not necessarily fibrillation. The latter is perhaps a more complex phenomenon in which several spatial and temporal irregularities might coexist. For this reason and for the time being, we do not attempt to answer Goldberger's question whether fibrillation is (or is not) chaos (14). Any subharmonic cardiac frequency regime (or "multupling" regime, as called by Ritzenberg et al. [13]) found in these experiments is probably similar to or the same kind as those reported by the latter authors (13) and commonly named in cardiovascular physiology and cardiology as "electrical alternans."

To illustrate theoretically the previously described period-doubling bifurcations, we can make use of the following simple unidimensional dynamic system,

$$X_{n+1} = C - X_n^2,$$

which was studied by Grebogi in 1987 (24). By iterating about 100 times this equation, say, with $C = 0.5$ and initial value $X_0 = 0$, the values of X tend progressively to a single stable value. Such solution (or orbit) corresponds to a period 1 (or order 0 bifurcation) similar to that observed in Figs. 2 *B* and 4 *A*, where the MAP amplitude does not change. Starting with the same initial condition as before and $C = 1.1$, after enough iterations, X will stabilize in two different values which correspond to a period 2 solution (or order 1 bifurcation). Figs. 3, *A–C*, and 4 *B* show precisely such case, in which two different amplitudes for the MAP signal are clearly depicted. If now we start again from the same initial condition X_0 but with $C = 1.3$, after sufficient iterations, four different values for X will be reached, showing a new bifurcation, this time of period 4 or order 2 bifurcation. Figs. 3 *D* and 4 *C* display this situation showing four amplitudes for the MAP signal. Finally, another iteration with $C = 1.4$ and the same X_0 will lead to a set of all different Xs because a very large number of bifurcations take place (order *n*). Figs. 3 *E* and 4 *D* would correspond to the latter case.

At present, a full understanding of the several and complex electrophysiological mechanisms has not been achieved. Our main objective would intend to answer the question of why the MAP amplitudes are periodically different. This may be due to the number of fibers that are depolarizing (change) in every cycle or to the action potentials of the fibers that periodically are functionally different. In both cases, we would obtain periodic differences in the MAP signal amplitudes. As far as it is known, this is still unexplained. In his postumous work in 1913, Mines (25), attributed the electrical and mechanical alternans to changes in the number of fibers that depolarize. However, Kremers attributed them to refractory period dispersion in the R and T waves of the ECG (23). On the other hand, periodic differences of the MAP amplitudes may be due to membrane nonlinear dynamics (26). The following reasons would support the latter explanation: (*a*) numerical integration of the Beeler and Reuter equation system presents sequences of amplitude period doubling and chaos (6, 7), (*b*) an experimental detection of a chaotic behavior in cultured cardiac cells was found by Guevara (12). Nevertheless, there is no conclusive experimental confirmation in ventricular tissue in situ. Interestingly enough, an autonomous nonoscillating system, as a perfused ventricle, shows qualitative dynamics similar to auto-oscillators which can be modeled by circle maps (8–10).

The trajectories shown in Fig. 6 are a bidimensional projection of a higher dimension attractor (probably chaotic). The chaotic attractor hypothesis is suggested by the band structure obtained from the bidimensional projection and also by the space-filling points in the Poincaré map. The existence of an approximately one-dimensional Poincaré map is suggested by the appearance of period-doubling bifurcations. However, so far it has not been demonstrated, perhaps because such a map is actually at least bidimensional.

A most interesting observation is that an autonomous nonoscillating system, as a perfused ventricle (where there is no proper frequency to compete with the external one), shows qualitative dynamics similar to spontaneously beating cells (12) and to auto-oscillators which can be modeled by circle maps (8–10). These observations agree with results obtained from nonoscillatory sheep Purkinje fibers when rhythmically driven (26). The observed period-doubling sequences leading to chaos would indicate that fibrillation may be preceded by period-doubling and higher order phase-locking regimes. In both, there were evidences of an increase in the effective dimensionality of the system.

In summary, the MAP signal temporal series irregularity, the broadband noise at low frequency in the power

spectrum, the rapid autocorrelation decay, the space-filling points in the Poincaré maps, the period-doubling sequences, the band-like compression of the bidimensional phase portrait trajectories and the sensivitivity to initial conditions are supporting evidence, if not proof, of a universal chaotic behavior in the toad ventricular electrical activity. The possibility of a low-dimensional chaotic attractor in its local dynamics ought to be confirmed by other types of measurements, such as the Hausdorff dimension or a lower bound for the Kolmogorov entropy.

It is concluded that (*a*) bifurcations of order one and two and irregular behavior detected in the MAP signal amplitude are evidences of universal chaotic dynamics in cardiac tissue; (*b*) there are no qualitative differences in the dynamics of the in situ (oscillating) and nonoscillating (perfused) toad ventricles; and (*c*) fibrillation seems to be related to chaotic behavior, but whether they are similar or equivalent phenomena still remains to be seen.

We would like to thank Mr. F. Dürig, Mr. M. Magnasco, Mr. F. A. Hirsch, and Mrs. L. Troyano for their help in different stages of the preparation of this paper. It was communicated to the World Congress on Medical Physics and Biomedical Engineering, held in San Antonio, TX, 6–12 August 1988 (see 1988. *Phys. Med. Biol.* 33(Suppl. I):230, [Abstr. BE7-E2]). Besides, the paper was presented and discussed in seminars given at the Hillenbrand Biomedical Engineering Center, Purdue University (West Lafayette, IN, 18 August 1988), Department of Physics and Astronomy, Vanderbilt University (Nashville, TN, 22 August 1988), and Department of Biomedical Engineering, Johns Hopkins University (Baltimore, MD, 26 August 1988).

Supported by grants from Consejo Nacional de Investigaciones Científicas y Técnicas, Secretaría de Estado de Ciencia y Técnica, and Consejo de Investigaciones de la Universidad Nacional de Tucumán.

Received for publication 11 October 1988 and in final form 3 February 1989.

REFERENCES

1. Surawicz, B. 1985. Ventricular fibrillation. *J. Am. Coll. Cardiol.* 5:43B–54B.
2. Best, E. N. 1979. Null space in the Hodgkin-Huxley equations. A critical test. *Biophys. J.* 27:87–104.
3. Jalife, J., and C. Antzelevitch. 1979. Phase resetting and annihilation of pacemaker activity in cardiac tissue. *Science (Wash. DC).* 206:695–697.
4. Guevara, M. R., and L. Glass. 1982. Phase locking, period doubling bifurcations and chaos in a mathematical model of a periodically driven oscillator: a theory for the entrainment of biological oscillator and the generation of cardiac dysrhythmias. *J. Math. Biol.* 14:1–23.
5. Beeler, G. B., and H. Reuter. 1977. Reconstruction of the action potential of ventricular myocardial fibres. *J. Physiol. (Lond.).* 268:177–210.
6. Chay, T. R., and Y. S. Lee. 1985. Phase resetting and bifurcation in the ventricular myocardium. *Biophys. J.* 47:641–651.
7. Jensen, J. H., P. L. Chistiansen, A. C. Scott, and O. Skougaard. 1984. Chaos in the Beeler-Reuter system for the action potential of ventricular myocardial fibres. *Physica.* 13D:269–277.
8. González, D. L., and O. Piro. 1983. Chaos in a nonlinear driven oscillator with exact solution. *Phys. Rev. Lett.* 50:870–872.
9. González, D. L., and O. Piro. 1984. One-dimensional Poincaré map for a non-linear driven oscillator: analytical derivation and geometrical properties. *Phys. Lett.* 101A:455–458.
10. González, D. L., and O. Piro. 1984. Disappearance of chaos and integrability in an externally modulated nonlinear oscillator. *Phys. Rev.* A 30:2788–2790.
11. González, D. L., and O. Piro. 1985. Symmetric kicked self-oscillators: iterated maps, strange attractors, and symmetry of the phase-locking Farey hierarchy. *Phys. Rev. Lett.* 55:17–20.
12. Guevara, M. R., L. Glass, and A. Shrier. 1981. Phase locking, period-doubling bifurcation, and irregular dynamics in periodically stimulated cardiac cells. *Science (Wash. DC).* 214:1350–1353.
13. Ritzenberg, A. L., D. R. Adam, and R. J. Cohen. 1984. Period multuplying-evidence for nonlinear behavior of the canine heart. *Nature (Lond.)* 307:159–161.
14. Goldberger, M. D., V. Bahargava, B. J. West, and A. J. Mandell. 1986. Some observations on the question: is ventricular fibrillation "chaos"? *Physica.* 19D:282–289.
15. Cranefield, P. F., J. A. E. Eyster, and W. E. Gilson. 1951. Electrical characteristics of injury potentials. *Am. J. Physiol.* 167:450–456.
16. Hoffman, B. F., P. F. Cranefield, E. Lepeschkin, B. Surawicz, and H. C. Herrlich. 1958. Comparison of cardiac monophasic action potentials recorded by intracellular and suction electrodes. *Am. J. Physiol.* 196:1297.
17. Tarr, M., and N. Sperelakis. 1964. Weak electrotonic interaction between contiguous cardiac cells. *Am. J. Physiol.* 207:691–700.
18. Schanne, O. F., and E. Ruiz P.-Ceretti. 1978. Impedance Measurements in Biological Cells. John Wiley & Sons, New York. 205–207.
19. Packard, N., J. P. Crutchfield, J. D. Farmer, and R. S. Shaw. 1980. Geometry from a time series. *Phys. Rev. Lett.* 45:712–716.
20. Farmer, J. D. 1982. Chaotic attractor of an infinite-dimensional system. *Physica.* 4D:366.
21. Hao Bai-Lin. 1984. *Chaos.* World Scientific Publishing Co., Singapore. 576 pp.
22. Savino, G. V., and M. E. Valentinuzzi. 1988. Ventricular fibrillation-defibrillation in the toad *Bufo paracnemis. Int. J. Cardiol.* 19:19–25.
23. Kremers, M. S., J. M. Miller, and M. E. Josephson. 1985. Electrical alternans in wide complex tachycardias. *Am. J. Cardiol.* 56:305–308.
24. Grebogi, C., E. Ott, and J. A. Yorke. 1987. Chaos, strange attractors, and fractal basin boundaries in nonlinear dynamics. *Science (Wash. DC).* 238:632–638.
25. Mines, G. R. 1913. On dynamic equilibrium in the heart. *J. Physiol.* 46:349–383.
26. Chialvo, D. R., and J. Jalife. 1987. Non-linear dynamics of cardiac excitation and impulse propagation. *Nature (Lond.).* 330:749–752.